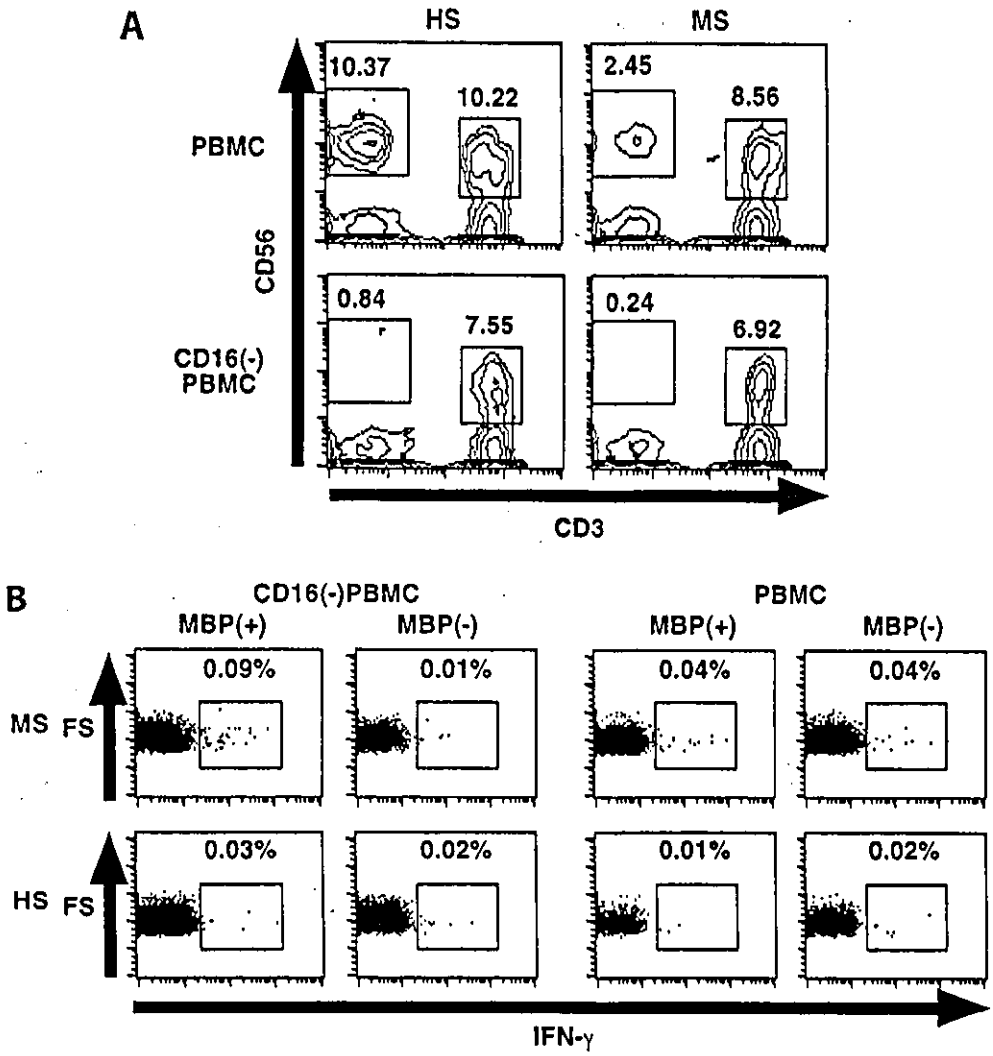

Fig. 3 Depletion of CD16$^+$ cells also allows detection of MBP-specific memory T cells in 'CD95$^+$ NK-high' multiple sclerosis. (A) Changes in the frequency of CD56$^+$ NK cells and CD56$^+$ NKT cells after deleting CD16$^+$ cells. Using CD16 microbeads, we deleted CD16$^+$ cells from PBMCs from two 'CD95$^+$ NK-high' patients and from two healthy subjects. The cells were stained with anti-human CD3-FITC and anti-CD56-PC5 to check the proportion of CD56$^+$ NK cells and CD56$^+$ T cells before and after CD16$^+$ cell depletion (upper versus lower panels). Shown are the results of a representative pair of multiple sclerosis and healthy subjects. (B) CD16$^+$-cell-depleted PBMCs from 'CD95$^+$ NK-high' multiple sclerosis responded rapidly to MBP. Using the same PBMC samples (CD16$^+$ or CD16$^-$), we conducted the IFN-γ secretion assay as described in Fig. 2A. This figure shows the result of the representative pair of multiple sclerosis patients and healthy subjects.

the TCC as read-out, we compared the whole PBMCs and the NK cell-deleted PBMCs for the ability to present whole MBP to the autologous TCC. We found that the whole PBMCs did not differ from the NK-deleted PBMCs in the ability to induce MBP-driven proliferation of TCC (Fig. 4A). However, the proportion of IFN-γ-secreting T cells among the TCC increased significantly when the NK cell-depleted PBMCs were used as antigen presenting cells (APC) (Fig. 4B). We also noticed a significant elevation of IFN-γ in the culture supernatant along with the increase of IFN-γ-secreting T cells (Fig. 4C). However, neither TNF-α nor IL-2 production was enhanced by NK cell depletion. These results support the view that NK cells from 'CD95$^+$ NK-high' multiple sclerosis regulate autoimmune T cells by inhibiting the T cell production of IFN-γ.

Discussion

It is generally held that relapse of multiple sclerosis represents the destructive CNS inflammation triggered by recently activated autoimmune T cells. In other words, pathogenic autoimmunity is apparently active during clinical relapse, which can be objectively defined by clinical status as well as MRI findings. In contrast, remission of multiple sclerosis, which is chiefly determined by exclusion of active inflammation in the CNS, may probably cover a wider range of disease states.

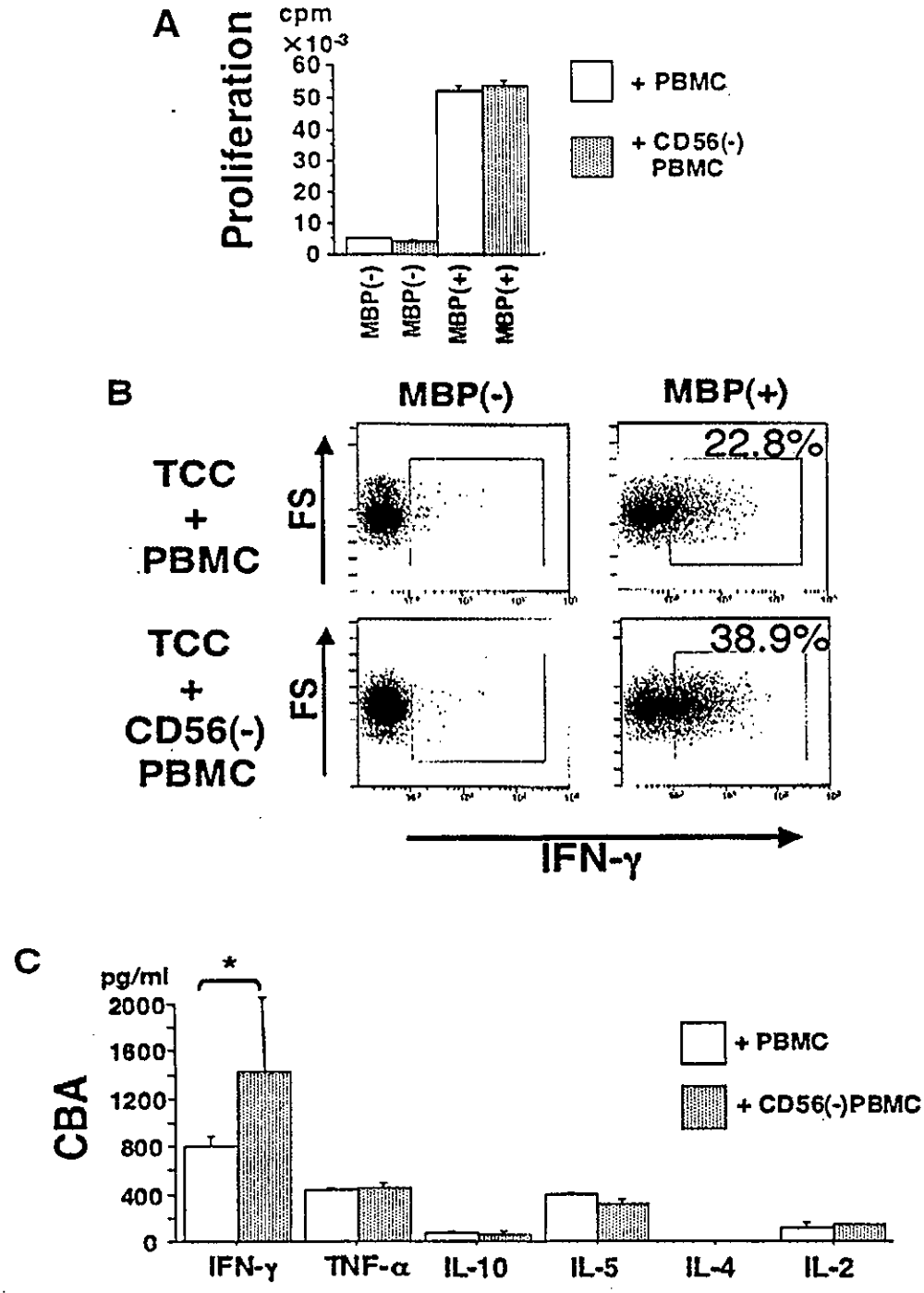

Fig. 4 Depletion of NK cells augments the antigen-presenting potential of PBMCs from 'CD95$^+$ NK-high' multiple sclerosis. (A) Effect of NK-cell deletion on the proliferation of MBP-specific TCC. We established three MBP-specific TCC from a 'CD95$^+$ NK-high' patient, and evaluated the proliferative response of the clone cells to MBP (10 μg/ml) in the presence of fresh autologous PBMCs [+ PBMC] or NK-deleted PBMCs [+ CD56 (−) PBMC]. This is a representative result of three TCC, which yielded essentially the same results. Data represent mean ±SD of quadruplicate cultures. (B) Effect of NK cell deletion on IFN-γ secretion by the MBP-specific TCC. MBP-specific TCC were cultured with or without MBP for 8 h in the presence of autologous PBMCs (upper panels) or of the autologous PBMCs depleted for CD56$^+$ NK cells (lower panels). We then conducted the cytokine secretion assay to detect IFN-γ-positive cells. Red dots indicate IFN-γ-secreting cells among CD4$^+$CD3$^+$PI$^-$ cells; blue dots represent IFN-γ-negative CD4$^+$CD3$^+$PI$^-$ T cells. The values (%) represent the frequency of IFN-γ-secreting cells among CD4$^+$CD3$^+$PI$^-$ cells. We conducted the assay with three TCC, which yielded essentially the same results. FS = forward scatter. (C) Effect of NK cell depletion on cytokine release by TCC into culture medium. The TCC were stimulated with MBP for 48 h in the presence of autologous PBMCs or NK-depleted PBMCs. Then we measured the concentrations of IFN-γ, TNF-α, IL-10, IL-5, IL-4 and IL-2 in the supernatants, using ELISA and CBA. Both assays yielded essentially the same results, and here we show the result of a CBA assay. Data represent mean ± SD. The Mann–Whitney *U*-test was used for statistical analysis. *$P < 0.05$. We conducted the assay with three TCC, which yielded essentially the same results.

The present results show that multiple sclerosis patients in remission can be divided at least into two subgroups, 'CD95$^+$ NK-high' and 'CD95$^+$ NK-low', based on the frequency of CD95$^+$ cells among NK cells. Furthermore, our functional analysis combining NK cell deletion and stimulation with MBP has indicated that the two subgroups differ significantly with regard to the responsiveness of the MBP-specific memory T cells to MBP in the absence of NK cells. Namely, after deleting CD56$^+$ NK cells, we saw a rapid induction of IFN-γ-secreting, anti-MBP T cells in 'CD95$^+$ NK-high' multiple sclerosis, whereas such a rapid response to MBP was not seen in 'CD95$^+$ NK-low' multiple sclerosis or healthy subjects. This result is in harmony with the previous results that clonally expanded MBP-specific T cells can be detected in a majority of multiple sclerosis patients (Zhang *et al.*, 1994; Smeltz *et al.*, 1999), and indicates that patients with an increased number of the autoimmune T cells may have the 'CD95$^+$ NK-high' phenotype during remission. Thus, the frequency of CD95$^+$ NK cells correlates with the frequency of MBP-reactive memory T cells and may serve as a useful marker to evaluate the immunological status of multiple sclerosis during remission.

The role of NK cells in the regulation of MBP-specific T cells was further strengthened by the demonstration that deletion of CD16$^+$ cells also enabled detection of memory MBP-specific T cells. Because we confirmed that depletion of the CD16$^+$ cells would greatly reduce the number of NK cells but did not significantly reduce CD56$^+$CD3$^+$ NK T cells, the role of the NK T cells in the regulation was excluded.

We have previously described that the 'CD95$^+$ NK-low' phenotype could also be seen in multiple sclerosis patients during relapse. However, the 'CD95$^+$ NK-low' phenotype in MS-rel was not persistent, but the 'CD95$^+$ NK-high' phenotype could be regained in a month or so along with clinical recovery. This fact raised the possibility that 'CD95$^+$ NK-low' MS-rem may represent an active state of multiple sclerosis, contrary to our speculation. To evaluate this possibility, we examined three patients with MS-rem for the 'CD95$^+$ NK-high/low' phenotype every 4–6 weeks, and found that they maintained the 'CD95$^+$ NK-low' phenotype for longer than several months (data not shown). This is in a striking contrast to the transient appearance of the 'CD95$^+$ NK-low' phenotype during relapse. Together with the clinical observations that these patients were in a very stable condition with minimal neurological disability, we estimate the disease condition in 'CD95$^+$ NK-low' MS-rem to be truly inactive and distinct from MS-rel.

It is of note that IFN-γ-secreting T cells could be identified as early as 8 h after stimulation with MBP in the absence of NK cells. This result implies that the NK cells should interact with the autoimmune T cells shortly after antigen stimulation to regulate very early T cell response. To account for such a rapid regulation by NK cells, we speculate that the regulatory NK cells may detect the subtle change of the autoimmune T cells during the early stage of activation. At present, very little is known about the molecular basis of T cell–NK cell interaction. However, it is obvious that NK cells must interact with T cells in an antigen-non-specific fashion, as they do not express highly variable receptors like T cell antigen receptors. Our results indicate that attempts to identify the ligand and receptors involved in T cell–NK interactions are very rewarding.

It is currently speculated that activation of autoimmune T cells could occur in response to microbial proteins whose sequence has a significant homology to the self-peptide (Steinman, 2001). We predict that the increased MBP-reactive Th1 cells in the 'CD95$^+$ NK-high' patients will most likely respond to microbial peptides mimicking MBP from time to time. However, counter-regulatory NK cells would maintain the clinical silence by actively suppressing activation of the autoimmune T cells that might lead to destructive CNS inflammation (Fig. 5). We then imagine that the clinical silence in the 'CD95$^+$ NK-high' patients could readily be disrupted when NK cells are numerically or functionally altered by exogenous or endogenous factors independent of multiple sclerosis (Wu *et al.*, 2000). In contrast, the clinical remission in 'CD95$^+$ NK-low' multiple sclerosis appears to be stable, as they are expected to possess much lower numbers of MBP-specific memory T cells, which does not necessitate the active

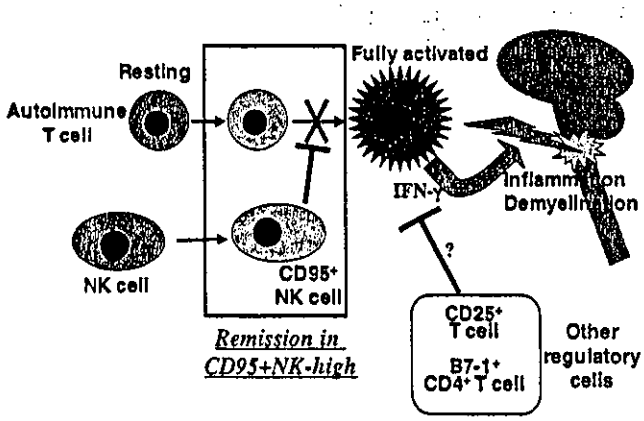

Fig. 5 The role of NK cells in 'CD95$^+$ NK-high' multiple sclerosis. As described in the text, the 'CD95$^+$ NK-high' patients are characterized by a concurrent increase of memory autoimmune T cells and CD95$^+$ NK cells. In the sense that memory autoimmune T cells cannot be detected in other patients in remission ('CD95$^+$ NK-low') even after NK cell depletion, we describe the immunological status of the 'CD95$^+$ NK-high' as a 'smouldering' state rather than 'remission'. Given that T cell recognition is much more promiscuous than previously anticipated, we imagine that autoimmune T cells in the 'CD95$^+$ NK-high' patients would respond to exogenous self-mimicking peptides from time to time. However, our results indicate that the CD95$^+$ NK cells could detect the early sign of T cell activation and then interact with autoimmune T cells to prohibit their full activation. Once this delicate control by NK cells is disrupted, the autoimmune T cells could be fully activated in response to the self-mimicking peptides. The fully activated T cells may be controlled by other regulatory cells such as CD4$^+$CD25$^+$ T cells (Sakaguchi *et al.*, 2001) or B7-1$^+$CD4$^+$ T cells (Kipp *et al.*, 2000). However, it is difficult to predict how efficiently the regulatory T cells may control the activated autoimmune T cells in individual cases.

engagement of regulatory NK cells. If these premises hold true, we may consider that the 'CD95$^+$ NK-high' patients are at a greater risk than 'CD95$^+$ NK-low' of developing relapses when exposed to potentially dangerous microbes that have cross-reactive epitopes. To describe the immunological status in 'CD95$^+$ NK-high', which seems to be more active than the 'CD95$^+$ NK-low', it might be appropriate to use the term 'smouldering' state rather than 'remission'.

After determining the presence of the 'CD95$^+$ NK-high' and 'CD95$^+$ NK-low' phenotypes in the patients with MS-rem, an important question might be whether the 'CD95$^+$ NK-high/-low' phenotype correlates with some clinical parameters or disease course. We speculated that 'CD95$^+$ NK-low' might be clinically less active than 'CD95$^+$ NK-high', when evaluated retrospectively. However, it might take time and would require a large number of patients to verify this postulate, taking the heterogeneity and chronic nature of the illness into consideration. Furthermore, it is of note that the 'CD95$^+$ NK-high' or '-low' phenotype appears to be interchangeable. For example, two of the patients who were examined for the memory T cell frequency showed the 'CD95$^+$ NK-low' phenotype in the first examination, but were found to have the 'CD95$^+$ NK-high' phenotype when examined 1 year later (Table 1). The phenotype switch in these patients was associated with an increase in the frequency of MBP-reactive memory T cells. We speculate that activity of multiple sclerosis may have been increased in these patients during the 1-year interval, although it is too early to draw any conclusions from the analysis of two patients.

Conversely, we have recently seen an opposing phenotype switch (from the 'CD95$^+$ NK-high' to 'CD95$^+$ NK-low') in two other patients. The frequency of CD95$^+$ cells among NK cells was >46.0% in both cases in the initial examinations, but the latest test showed normal values (27.4% and 10.0%). Although the patients appeared to be in the state of remission at the last examination, they developed serious signs of acute exacerbation 2 days later. As stated above, a transient switch from 'CD95$^+$ NK-high' to 'CD95$^+$ NK-low' could occur during relapse. Therefore, we speculate that the phenotype switch from 'high' to 'low' may be triggered by the very early events leading to clinical relapse. However, it is also possible that the reduction of the CD95$^+$ NK cells might have been triggered by multiple sclerosis-independent factors, such as infection or stress, and that this led to the occurrence of the relapse in these patients. This speculation is supported by the fact that a number of physiological conditions can alter NK cell number and/or function, and that CD95$^+$ NK cells tend do die more rapidly in culture than CD95$^-$ NK cells (our unpublished data). In future, it will be worthwhile to examine more systematically whether the phenotype switch may be the earliest marker to detect occurrence of relapse.

As Japanese neurologists have traditionally stressed that multiple sclerosis in Japan might be quite unique in immunopathology, it is theoretically possible that the regulatory function of CD95$^+$ NK cells reflects the uniqueness of Japanese multiple sclerosis and that the T cell–NK cell interaction is not operative in Caucasian multiple sclerosis. However, recent studies suggest that the frequency of pure optic-spinal form of multiple sclerosis linked with Japanese patients (Misu *et al.*, 2002) is drastically declining, possibly due to change in lifestyle or environmental factors in Japan (Yamamura, 2002; Houzen *et al.*, 2003). Reflecting this fact, the patients randomly recruited in this study did not have optic-spinal multiple sclerosis, and all had brain lesions similar to those found in Western multiple sclerosis. We therefore speculate that our experimental results will be reproduced in Caucasian patients in the future.

In summary, we have revealed that multiple sclerosis patients in remission have either 'CD95$^+$ NK-high' or 'CD95$^+$ NK-low' phenotype, and that 'CD95$^+$ NK-high' patients have a higher frequency of memory autoimmune T cells and have more active multiple sclerosis than 'CD95$^+$ NK-low' patients. Our *ex vivo* assay has demonstrated that 'CD95$^+$ NK-high' patients possess NK cells that actively inhibit activation of memory autoimmune T cells. In the sense that clinical silence depends on the functional regulatory NK cells, the condition of 'CD95$^+$ NK-high' is thought to be so unstable, as could be expressed by the term 'smouldering'. As such, evaluation of the NK cell functions and phenotypes in multiple sclerosis gives us a new insight into the autoimmune pathogenesis of multiple sclerosis, encouraging further efforts to clarify the NK cell–T cell interactions.

Acknowledgements

We wish to thank Christian Rochford for critical reading of this manuscript. This work was supported by grants from the Ministry of Health, Labor and Welfare of Japan and from the Organization for Pharmaceutical Safety and Research.

References

Allegretta M, Nicklas JA, Sriram S, Albertini RJ. T cells responsive to myelin basic protein in patients with multiple sclerosis. Science 1990; 247: 718–21.

Bieganowska KD, Ausubel LJ, Modabber Y, Slovik E, Messersmith W, Hafler DA. Direct *ex vivo* analysis of activated, Fas-sensitive autoreactive T cells in human autoimmune disease. J Exp Med 1997; 185: 1585–94.

Bielekova B, Goodwin B, Richert N, Cortese I, Kondo T, Afshar G, et al. Encephalitogenic potential of the myelin basic protein peptide (amino acids 83–99) in multiple sclerosis: results of a phase II clinical trial with an altered peptide ligand. Nat Med 2000; 6: 1167–75.

Bjartmar C, Trapp BD. Axonal and neuronal degeneration in multiple sclerosis: mechanisms and functional consequences. Curr Opin Neurol 2001; 14: 271–8.

Cook EB, Stahl JL, Lowe L, Chen R, Morgan E, Wilson J, et al. Simultaneous measurement of six cytokines in a single sample of human tears using microparticle-based flow cytometry: allergics vs. non-allergics. J Immunol Methods 2001; 254: 109–18.

Das MP, Nicholson LB, Greer JM, Kuchroo VK. Autopathogenic T helper cell type 1 (Th1) and protective Th2 clones differ in their recognition of the autoantigenic peptide of myelin proteolipid protein. J Exp Med 1997; 186: 867–76.

Deibler GE, Martenson RE, Kies MW. Large scale preparation of myelin basic protein from central nervous tissue of several mammalian species. Prep Biochem 1972; 2: 139–65.

Deibler GE, Burlin TV, Stone AL. Three isoforms of human myelin basic protein: purification and structure. J Neurosci Res 1995; 41: 819–27.

Duda PW, Schmied MC, Cook SL, Krieger JI, Hafler DA. Glatiramer acetate (Copaxone) induces degenerate, Th2-polarized immune responses in patients with multiple sclerosis. J Clin Invest 2000; 105: 967–76.

Houzen H, Niino M, Kikuchi S, Fukazawa T, Nogoshi S, Matsumoto H, et al. The prevalence and clinical characteristics of MS in northern Japan. J Neurol Sci 2003; 211: 49–53.

Illés Z, Kondo T, Yokoyama K, Ohashi T, Tabira T, Yamamura T. Identification of autoimmune T cells among *in vivo* expanded CD25 + T cells in multiple sclerosis. J Immunol 1999; 162: 1811–7.

Jacobs R, Hintzen G, Kemper A, Beul K, Kempf S, Behrens G, et al. $CD56^{bright}$ cells differ in their KIR repertoire and cytotoxic features from $CD56^{dim}$ NK cells. Eur J Immunol 2001; 31: 3121–7.

Kipp B, Bar-Or A, Gausling R, Oliveira EM, Fruhan SA, Stuart WH, et al. A novel population of B7-1 + T cells producing intracellular IL-4 is decreased in patients with multiple sclerosis. Eur J Immunol 2000; 30: 2092–100.

Lovett-Racke AE, Trotter JL, Lauber J, Perrin PJ, June CH, Racke MK. Decreased dependence of myelin basic protein-reactive T cells on CD28-mediated costimulation in multiple sclerosis patients. A marker of activated/memory T cells. J Clin Invest 1998; 101: 725–30.

Manz R, Assenmacher M, Pfluger E, Miltenyi S, Radbruch A. Analysis and sorting of live cells according to secreted molecules, relocated to a cell-surface affinity matrix. Proc Natl Acad Sci USA 1995; 92: 1921–5.

Martin R, Howell MD, Jaraquemada D, Flerlage M, Richert J, Brostoff S, et al. A myelin basic protein peptide is recognized by cytotoxic T cells in the context of four HLA-DR types associated with multiple sclerosis. J Exp Med 1991; 173: 19–24.

Martin R, McFarland HF, McFarlin DE. Immunological aspects of demyelinating diseases. Annu Rev Immunol 1992; 10: 153–87.

Matsumoto Y, Kohyama K, Aikawa Y, Shin T, Kawazoe Y, Suzuki Y, et al. Role of natural killer cells and TCR γδ T cells in acute autoimmune encephalomyelitis. Eur J Immunol 1998; 28: 1681–8.

McDonald WI, Compston A, Edan G, Goodkin D, Hartung HP, Lublin FD, et al. Recommended diagnostic criteria for multiple sclerosis: guidelines from the International Panel on the diagnosis of multiple sclerosis. Ann Neurol 2001; 50: 121–7.

Misu T, Fujihara K, Nakashima I, Miyazawa I, Okita N, Takase S, et al. Pure optic-spinal form of multiple sclerosis in Japan. Brain 2002; 125: 2460–8.

Neuhaus O, Farina C, Yassouridis A, Wiendl H, Then Bergh F, Dose T, et al. Multiple sclerosis: comparison of copolymer-1-reactive T cell lines from treated and untreated subjects reveals cytokine shift from T helper 1 to T helper 2 cells. Proc Natl Acad Sci USA 2000; 97: 7452–7.

Ohashi T, Yamamura T, Inobe J, Kondo T, Kunishita T, Tabira T. Analysis of proteolipid protein (PLP)-specific T cells in multiple sclerosis: identification of PLP95-116 as an HLA-DR2,w15-associated determinant. Int Immunol 1995; 7: 1771–8.

Olivares-Villagomez D, Wang Y, Lafaille JJ. Regulatory $CD4^+$ T cells expressing endogenous T cell receptor chains protect myelin basic protein-specific transgenic mice from spontaneous autoimmune encephalomyelitis. J Exp Med 1998; 188: 1883–94.

Ota K, Matsui M, Milford EL, Mackin GA, Weiner HL, Hafler DA. T-cell recognition of an immunodominant myelin basic protein epitope in multiple sclerosis. Nature 1990; 346: 183–7.

Panitch HS, Hirsch RL, Schindler J, Johnson KP. Treatment of multiple sclerosis with gamma interferon: exacerbations associated with activation of the immune system. Neurology 1987; 37: 1097–102.

Peritt D, Robertson S, Gri G, Showe L, Aste-Amezaga M, Trinchieri G. Differentiation of human NK cells into NK1 and NK2 subsets. J Immunol 1998; 161: 5821–4.

Pette M, Fujita K, Wilkinson D, Altmann DM, Trowsdale J, Giegerich G, et al. Myelin autoreactivity in multiple sclerosis: recognition of myelin basic protein in the context of HLA-DR2 products by T lymphocytes of multiple sclerosis patients and healthy donors. Proc Natl Acad Sci USA 1990; 87: 7968–72.

Poser CM, Paty DW, Scheinberg L, McDonald WI, Davis FA, Ebers GC, et al. New diagnostic criteria for multiple sclerosis: guidelines for research protocols. Ann Neurol 1983; 13: 227–31.

Sakaguchi S, Sakaguchi N, Shimizu J, Yamazaki S, Sakihama T, Itoh M, et al. Immunologic tolerance maintained by $CD25^+$ $CD4^+$ regulatory T cells: their common role in controlling autoimmunity, tumor immunity, and transplantation tolerance. Immunol Rev 2001; 182: 18–32.

Scholz C, Patton KT, Anderson DE, Freeman GJ, Hafler DA. Expansion of autoreactive T cells in multiple sclerosis is independent of exogenous B7 costimulation. J Immunol 1998; 160: 1532–8.

Smeltz RB, Wolf NA, Swanborg RH. Inhibition of autoimmune T cell responses in the DA rat by bone marrow-derived NK cells *in vitro*: implications for autoimmunity. J Immunol 1999; 163: 1390–7.

Steinman L. Multiple sclerosis: a two-stage disease. Nat Immunol 2001; 2: 762–4.

Takahashi K, Miyake S, Kondo T, Terao K, Hatakenaka M, Hashimoto S, et al. Natural killer type 2 bias in remission of multiple sclerosis. J Clin Invest 2001; 107: R23–9.

Wu W, Yamaura T, Murakami K, Murata K, Matsumoto K, Watanabe H, et al. Social isolation stress enhanced liver metastasis of murine colon 26-L5 carcinoma cells by suppressing immune responses in mice. Life Sci 2000; 66: 1827–38.

Yamamura T. Hypothetical view on the environmental factors, Th1/Th2 balance, and disease phenotype of MS/EAE. [Japanese]. Rinsho Shinkeigaku 2002; 42: 1201–3.

Zhang B, Yamamura T, Kondo T, Fujiwara M, Tabira T. Regulation of experimental autoimmune encephalomyelitis by natural killer (NK) cells. J Exp Med 1997; 186: 1677–87.

Zhang J, Markovic-Plese S, Lacet B, Raus J, Weiner HL, Hafler DA. Increased frequency of interleukin 2-responsive T cells specific for myelin basic protein and proteolipid protein in peripheral blood and cerebrospinal fluid of patients with multiple sclerosis. J Exp Med 1994; 179: 973–84.

Interferon β-responsive inclusion body myositis in a hepatitis C virus carrier

Y. Yakushiji, MD; J. Satoh, MD; M. Yukitake, MD; K. Yamaguchi, MD; I. Nakamura, MD; I. Nishino, MD; and Y. Kuroda, MD

Although an immune-mediated theory has been proposed for the pathogenesis of inclusion body myositis (IBM),[1,2] immunosuppressive treatment is not beneficial. We report a case of IBM occurring in a hepatitis C virus (HCV) carrier and showing improvement with the administration of a high dose of interferon-β (IFNβ).

Case report. A 68-year-old man was admitted because of generalized muscle weakness that progressed for over 8 years. Eight years earlier, he had developed chronic renal failure due to hyperuricemia and was treated with hemodialysis three times a week. At the induction of hemodialysis he was found to be a HCV carrier. Family history was unremarkable. General physical examination revealed no abnormalities other than hepatomegaly. On neurologic examination, symmetric weakness and atrophy of muscles were noted in all extremities. He was unable to stand, remain standing, or walk. Evaluation using manual muscle testing (MMT) scores included scores of 5 (normal) to 0 (complete paralysis). The results were as follows: shoulder-girdle muscles, 4; biceps and triceps, 4; wrist extensors and flexors, 4; finger extensors, 3; finger flexors, 0; quadriceps femoris, 0; and hamstrings, 4. Grasping power was 0 kg bilaterally.

Laboratory data included the following: aspartate aminotransferase, 38 IU/L (normal range: 10 to 30 IU/L); alanine aminotransferase, 19 IU/L (0 to 30 IU/L); creatine phosphokinase, 119 IU/L (60 to 240 IU/L); blood urea nitrogen, 38.9 mg/dL (5 to 20 mg/dL); and creatinine, 4.83 mg/dL (0.62 to 1.01 mg/dL). Antinuclear antibody, rheumatoid factors, and anti-Jo-1 antibody were all negative, but anti-HCV antibody was positive. Serum HCV titer was 516.2×10^3 copies/mL and genotype was categorized as type 1b. The MRI revealed severe symmetric atrophy of quadriceps femoris without abnormal intensity or gadolinium enhancement. Electromyography of the right biceps, triceps, quadriceps, and tibialis anterior muscles revealed poor interference patterns including low-amplitude short-duration potentials on voluntary contraction. Biopsy of the right biceps brachii muscle showed marked variations in fiber size, endomysial mononuclear cell infiltration (figure, A). Rimmed vacuoles were present in 4% of muscle fibers (figure, B). Electron microscopy detected tubulofilamentous nuclear inclusions. All of these findings supported a diagnosis of sporadic IBM.

To identify HCV infection in the muscle, frozen muscle tissues were processed for reverse transcription PCR analysis according to previously described methods.[3] HCV RNA positive-strand representing genomic HCV RNA was detected in both serum and muscle tissues of the patient, while HCV RNA negative-strand representing replicative intermediates of the virus was undetectable in both.

After providing informed consent, the patient was given an IV dose of 250 million international units (MIU) of natural IFNβ (Toray Co., Tokyo, Japan) over the course of 10 weeks. No serious adverse effects were observed. Following this therapy, serum HCV RNA levels were reduced to $< 0.5 \times 10^3$ copies/mL, accompanied by marked clinical improvement. He regained the ability to stand unaided and walk for more than several meters. MMT scores also showed improvement: shoulder-girdle muscles, 5; biceps and triceps, 5; wrist extensors and flexors, 5; finger extensors, 4; finger flexors, 2; quadriceps femoris, 2; and hamstrings, 4. Grasping power was 5 kg bilaterally.

Discussion. A recent randomized, double-blind, placebo-controlled study did not prove the efficacy of 30 microgram/week of IFNβ, IM injections for 24 weeks, for the treatment of IBM but observed a trend of IFN-associated improvement.[4] The authors concluded that studies with higher doses or longer durations of treatment are necessary. We report a case of sporadic IBM responding to IFNβ therapy. Although our patient was incapacitated, improvement of muscle strength was obtained after an IV dose of 250 MIU IFN over the course of 10 weeks. This was much higher than that of the controlled study (equivalent to 144 MIU over 24 weeks).

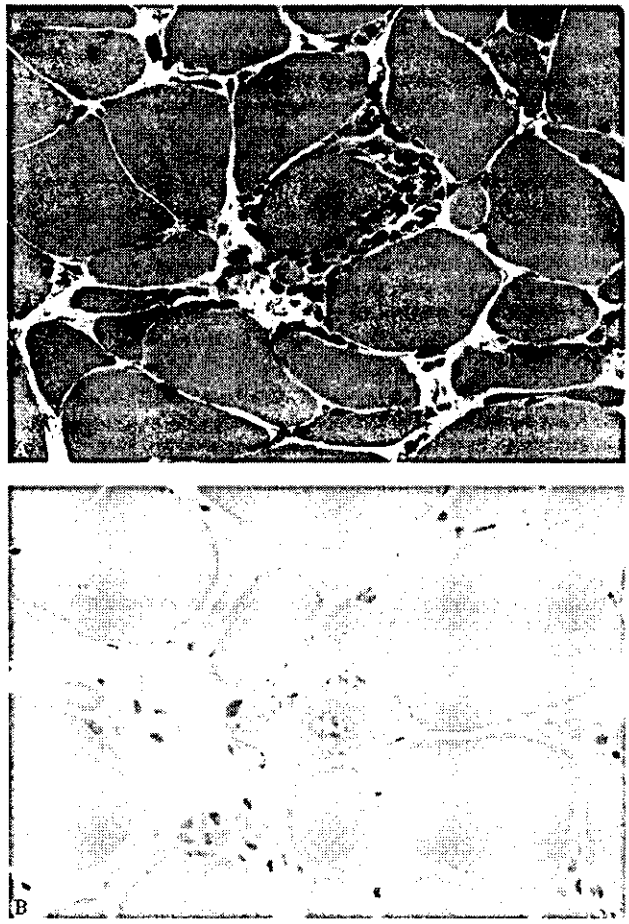

Figure. Biopsied specimen of the right biceps brachii muscle shows (A) marked variations in fiber size, endomysial mononuclear cell infiltration (H-E, ×460), and (B) rimmed vacuoles (Gomori-trichrome, ×460).

Our patient was a HCV carrier. Increasing evidence indicates that immune-mediated processes might cause IBM,[1,2] but the relationship between chronic viral infections and IBM is unclear. There is a report of occurrence of IBM in two HIV-1 carriers and one human T-cell lymphotrophic virus I carrier.[5] The authors reported that the viral genomes were detected in macrophages infiltrating around muscle fibers but not within the muscles in both conditions, suggesting that neither virus directly infects muscle cells. In this case we found that HCV RNA negative-strand representing replicative intermediates of the virus was not present in the muscle, but clinical improvement was associated with marked reduction in serum HCV RNA levels. Taken together, it is assumed that chronic viral infections might be involved as a trigger in the pathogenesis of IBM.

From The Division of Neurology (Drs. Yakushiji, Satoh, Yukitake, Yamaguchi, Nakamura, and Kuroda), Department of Internal Medicine, Saga University School of Medicine, Saga; and The Department of Neuromuscular Research (Dr. Nishino), National Institute of Neuroscience, Tokyo, Japan.

Received December 9, 2003. Accepted in final form March 11, 2004.

Address correspondence and reprint requests to Dr. Yusuke Yakushiji, Cerebrovascular Division, Department of Medicine, National Cardiovascular Center, 5-7-1 Fujishirodai, Suita, Osaka 565-8565, Japan; e-mail: yakushij@hsp.ncvc.go.jp

References

1. Pruitt JN, Showalter CJ, Engel AG. Sporadic inclusion body myositis: counts of different types of abnormal fibers. Ann Neurol 1996;39:139–143.
2. Amemiya K, Granger RP, Dalakas MC. Clonal restriction of T-cell receptor expression by infiltrating lymphocytes in inclusion body myositis persists over time. Studies in repeated muscle biopsies. Brain 2000;2030–2039.
3. Ueno Y, Kondo K, Kidokoro N, Kobayashi R, Kanaji K, Matsumu Hepatitis C infection and polymyositis. Lancet 1995;346:319–320.
4. The Muscle Study Group. Randomized pilot trial of βINF1a (Avon patients with inclusion body myositis. Neurology 2001;57:1566–15
5. Cupler EJ, Leon-Monzon M, Miller J, Semino-Mora C, Anderson Dalakas MC. Inclusion body myositis in HIV-1 and HTLV-1 in patients. Brain 1996;119:1887–1893.

Reversible paraneoplastic neuropathy associated with T-cell large granular lymphocyte leukemia

W.-Y. Au, MRCP, MD; W. Mak, MRCP, MD; S.-L. Ho, MD; S.-Y. Leung, MD; and Y.-L. Kwong, MD

T-cell large granular lymphocyte (T-LGL) leukemia is a rare leukemia originating from CD3$^+$, CD4$^-$, and CD8$^+$ T cells.[1] It is an indolent disease often associated with autoimmune manifestations, including rheumatoid arthritis, neutropenia, and pure red cell aplasia (PRCA).[2] Two unusual cases of T-LGL leukemia presented with prominent peripheral neuropathy, which improved significantly with successful leukemia treatment.

Case reports. Patient 1 was a 56-year-old man who sought treatment in 1996 for finger numbness, reduced dexterity, a severe glove and stocking sensory neuropathy extending to the elbow and knee, absent knee and ankle reflexes, but no motor weakness or ataxia. A blood count showed hemoglobin (Hb) 10.3 g/dL, white cell count (WCC) 3.5 × 10^9/L (60% of LGL), and platelet count (Plat) 210 × 10^9/L. The marrow was infiltrated by CD3$^+$, CD4$^-$, CD8$^+$, and CD56$^-$ T cells with clonal T-cell receptor-γ (TCRγ) gene rearrangement, confirming the diagn of T-LGL leukemia. The neuropathy did not respond to mon IV γ-globulin (0.5 g/kg). PRCA developed 1 year afterward. T ment with cyclosporine (CsA; 8 mg/kg) resulted in a remissio the PRCA within several months and gradual improvement o neuropathy. Tailing of CsA after 2 years led to a relapse o PRCA. Six monthly courses of FND (fludarabine 25 mg/m^2/d 3, mitoxantrone 10 mg/m^2/day × 1, and dexamethasone 20 mg × 5)[3] were administered, resulting in a sustained remission o T-LGL leukemia and PRCA. At 7-year follow-up evaluation was completely asymptomatic.

Patient 2 was a 53-year-old woman who sought treatmen fever and dyspnea in 1999. A blood count showed Hb 12.1 g WCC 17.4 × 10^9/L (33% LGL), and Plat 34 × 10^9/L. Ma examination showed infiltration by CD3$^+$, CD4$^-$, CD8$^+$, CD56$^-$ T cells with clonal TCRγ gene rearrangement, confirn the diagnosis of T-LGL leukemia. She developed progressive l eral lower limb weakness (grade 2 to 3), right foot drop, al ankle reflexes, impaired sensation to midthigh, and urinary r tion requiring catheterization. A urodynamic study showed al bladder tone. The CSF was normal. MRI from lower thorac lumbosacral region was also normal. Treatment with six mon

Table *Clinical, electrophysiologic, and histologic features of paraneoplastic neuropathy complicating two cases of T-cell large granul lymphocyte leukemia*

Gender/ age, y	Clinical state	Electrophysiologic studies	Sural nerve biopsy
M/56	Presentation	Sensory action potentials Attenuated in hands and feet Motor conduction velocity Normal	Semithin sections and ultrastructural examination Marked reduction in myelinated fibers an increase in endoneurial fibrosis, a fe actively degenerating myelinated and unmyelinated fibers, Schwann cell processes devoid of axons (bands of Büngner), and a few small axonal regenerative sprouts. Overall picture compatible with severe axonal degeneration. No leukemic infiltration.
	3-Year follow-up	Needle electromyogram Spontaneous denervational discharges with a neurogenic pattern of recruitment and broad polyphasic motor unit action potentials	
	7-Year follow-up	No deterioration	
F/53	Presentation	Sensory conduction velocities Mild slowing Distal motor latencies Marked prolongation Compound muscle action potential amplitude Attenuated Motor conduction velocity, F-minimal latencies Normal	Semithin section/ultrastructural study Moderate reduction in the number of myelinated fibers; large and medium myelinated fibers lined by abnormally t myelin sheath, with occasional fibers showing active myelin breakdown; occasional actively degenerating myelin fibers and axonal regenerative sprouts noted. The overall features were that of mixed active demyelination and axonal degeneration. No leukemic infiltration.
	3-Year follow-up	Marked improvement of all parameters	

Reprinted from:

IMMUNOLOGY 2004

MEDIMOND

INTERNATIONAL PROCEEDINGS

Dysregulation of Apoptosis-Regulatory Genes in Multiple Sclerosis

J.-i Satoh, M. Nakanishi and T. Yamamura

Department of Immunology, National Institute of Neuroscience, NCNP, 4-1-1 Ogawahigashi, Kodaira, Tokyo 187-8502, Japan

Summary

To clarify molecular mechanisms underlying multiple sclerosis (MS)-promoting autoimmune process, we have investigated a comprehensive gene expression profile of T cell and non-T cell fractions of peripheral blood mononuclear cells (PBMC) isolated from 72 MS patients and 22 age- and sex-matched healthy control (CN) subjects by analyzing a cDNA microarray. Among 1,258 genes examined, 173 genes in T cells and 50 genes in non-T cells were expressed differentially between MS and CN groups. Downregulated genes greatly outnumbered upregulated genes in MS. More than 80% of top 30 most significant genes were categorized into apoptosis signaling-related genes of both proapoptotic and antiapoptotic classes. They included upregulation in MS of orphan nuclear receptor Nurr1 (NR4A2), receptor-interacting serine/threonine kinase-2 (RIPK2), and silencer of death domains (SODD), and downregulation in MS of TNF-related apoptosis-inducing ligand (TRAIL), B-cell CLL/lymphoma-2 (BCL2), and death-associated protein-6 (DAXX). Furthermore, a number of the genes involved in DNA repair, replication and chromatin remodeling were downregulated in MS. By Northern blot analysis, the expression of the genes upregulated in MS was identified in cultured PBMC following stimulation with phorbol 12-myristate 13-acetate (PMA) and ionomycin (IOM), anti-CD3 monoclonal antibody (mAb), or interferon (IFN)-gamma. These results suggest that MS lymphocytes show a complex pattern of gene regulation which represents a counterbalance between promoting and preventing apoptosis and DNA damage.

Introduction

MS is mediated by Th1 cells whose development is triggered by a complex interplay of both genetic and environmental factors. Increasing evidence indicates that the elimination of autoreactive T cells by apoptosis, a common regulatory mechanism for normal development and homeostasis of the immune system, is impaired in MS (1). Previous studies showed that Fas, Fas ligand, and TRAIL expression is aberrantly regulated in PBMC and in active lesions of MS. However, these studies have focused on a limited range of apoptosis-signaling regulators. Application of DNA microarray technology has begun to give us new insights into the complexity of molecular interactions involved in the MS-promoting autoimmune process. Recently, we have studied the gene expression profile of T cells and non-T cells derived from MS before and after treatment with IFN-beta??2). IFN-beta altered the expression of 21 genes, including 9 with IFN-responsive promoter elements, thereby contributing to the therapeutic effects of IFN-beta in MS. Here we investigated a comprehensive gene expression profile of lymphocytes of 72 MS patients and 22 CN subjects by using a cDNA microarray.

Materials and Methods

The present study enrolled 72 Japanese, clinically active MS patients and age- and sex-matched 22 Japanese healthy CN subjects. No patients had a past history of treatment with interferons, glatiramer acetate or mitoxantrone. Total RNA was isolated from purified populations of CD3-positive T and CD3-negative non-T cells. The gene expression profile was studied by analyzing a 1,258 cDNA microarray (Hitachi Life Science) as described previously (2). The statistical significance of differentially expressed genes between MS and CN was evaluated by a regularized t test.

Results and Discussion

Among 1,258 genes examined, 173 genes in T cell fraction and 50 genes in non-T cell fraction were expressed differentially between 72 MS patients and 22 CN subjects. In T cell fraction, 25 genes were upregulated, while 148 genes were downregulated in MS. In non-T cell fraction, 11 genes were upregulated, while 39 genes were downregulated in MS. The great majority of top 30 significant genes in T cell and non-T cell fractions were categorized into apoptosis signaling-related genes of both proapoptotic and antiapoptotic classes (Fig. 1). They included upregulation in MS of NR4A2 in T, ICAM1, CXCL2, RIPK2, SODD, cell division cycle 42 (CDC42), and topoisomerase 2 alpha (TOP2A) in non-T, and downregulation in MS of TRAIL and polyADP-ribose polymer-

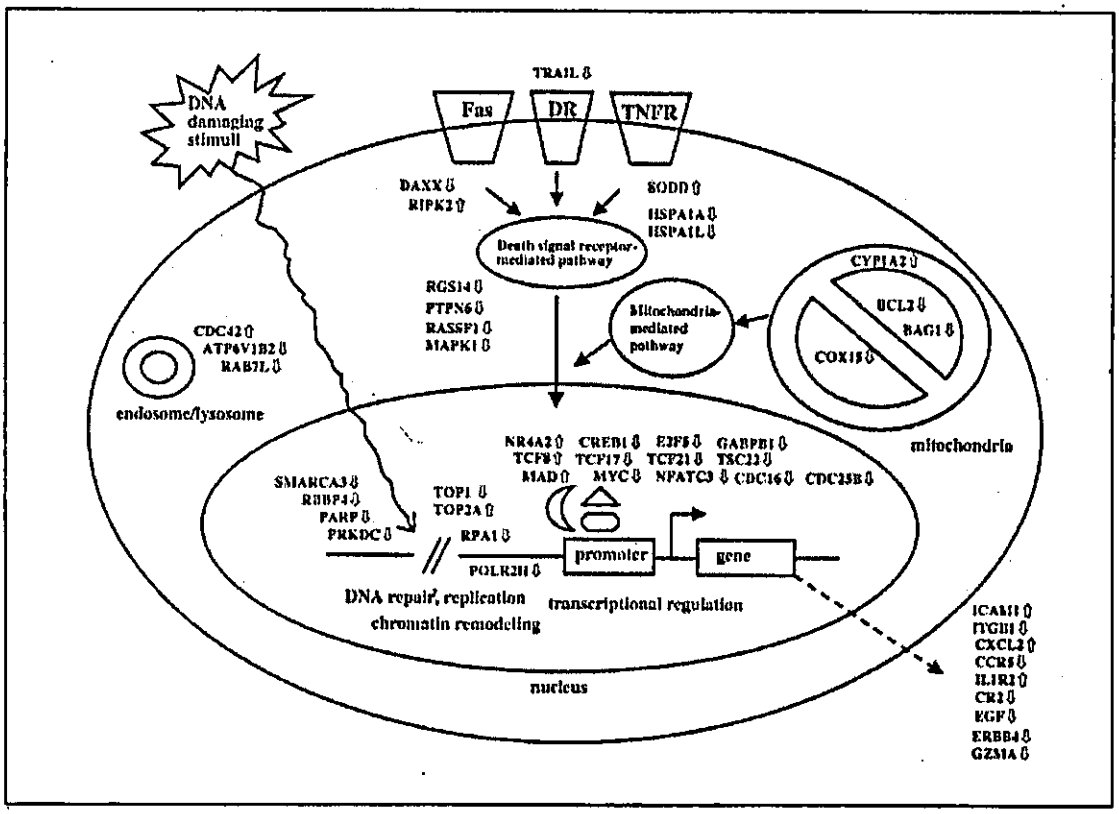

Fig. 1. Dysregulation of apoptosis signaling-related genes in MS lymphocytes. Top 30 differentially expressed genes in T cells or non-T cells between MS and CN groups, either upregulated or downregulated in MS, are shown.

ase (PARP) in T, BCL2 in non-T, and DAXX in both. To identify the stimuli inducing the expression of these genes, PBMC were exposed in vitro for varying periods to PMA plus IOM, anti-CD3 mAb, or IFN-?amma. PBMC exposed to PMA plus IOM showed the highest upregulation of NR4A2, ICAM1, RIPK2 and CXCL2, while treatment with anti-CD3 mAb exhibited more marked upregulation of CDC42, SODD and TOP2A. Thus, the genes upregulated in MS were expressed at significant levels in cultured PBMC in an activation- and stimulation-dependent manner. Previous studies showed that NR4A2 is upregulated in T cells during apoptosis. Overexpression of RIPK2 potentiates Fas-mediated apoptosis by activation of NF-kB, JNK and caspase-8. Th1 differentiation and cytokine production are severely impaired in RIPK2-deficient mice. SODD, by binding to the death domain of TNFR1 and death receptor DR3, blocks the post-receptor signal transduction. CDC42, a central member of the Rho-subfamily small GTPases, serves as a substrate for caspases in the Fas-signaling pathway. Topoisomerase is a nuclear enzyme that alters the topologic states of DNA, while PARP is a chromatin-associated enzyme that modifies nuclear proteins by polyADP-

ribosylation, thereby involved in maintenance of genomic stability. Our observations suggest that the gene expression pattern in PBMC of MS represents a counterbalance between promoting and preventing apoptosis and DNA damage of lymphocytes, which might be ceaselessly exposed to exogenous and endogenous apoptosis-inducing stimuli (Fig. 1).

Conclusions

Microarray analysis identified dysregulation of numerous apoptosis and DNA damage-regulatory genes in T cells and non-T cells of MS, reflecting a counterbalance between promoting and preventing apoptosis of lymphocytes in MS. Because the elimination of pathogenic autoreactive T cells is a pivotal step in the homeostasis of the immune system, dysregulation of apoptosis contributes to the autoimmune pathogenesis of MS.

References

1. ZIPP F et al. Immune (dys)regulation in multiple sclerosis: role of the CD95-CD95 ligand system. Immunol Today 20: 550-554, 1999.
2. KOIKE F et al. Microarray analysis identifies interferon ?eta-regulated genes in multiple sclerosis. J Neuroimmunol 139: 109-118, 2003.

JOBNAME: jnen 64#2 2005 PAGE: 1 OUTPUT: Mon December 27 15:05:18 2004
lww/jnen/93252/NEN19047

J Neuropathol Exp Neurol

Vol. 64, No. 2
February 2005
pp. 1–10

ORIGINAL ARTICLE

Nogo-A and Nogo Receptor Expression in Demyelinating Lesions of Multiple Sclerosis

Jun-Ichi Satoh, MD, PhD, Hiroyuki Onoue, MD, Kunimasa Arima, MD, PhD, and Takashi Yamamura, MD, PhD

Abstract:

A myelin-associated neurite outgrowth inhibitor, Nogo-A, plays a key role in inhibition of axonal regeneration following injury and ischemia in the central nervous system (CNS). Because axonal injury is a pathologic hallmark of multiple sclerosis (MS), we have investigated the expression of Nogo-A and its receptor NgR in four MS and 12 non-MS control brains by immunohistochemistry. Nogo-A expression was markedly upregulated in surviving oligodendrocytes at the edge of chronic active demyelinating lesions of MS and ischemic lesions of acute and old cerebral infarction, whereas NgR expression was greatly enhanced in reactive astrocytes and microglia/macrophages in these lesions when compared with their expression in the brains of neurologically normal controls. Nogo-A and NgR were also identified in a subpopulation of neurons. In contrast, Nogo-A was undetectable in reactive astrocytes and microglia/macrophages and NgR was not expressed on oligodendrocytes in any cases examined. Western blot analysis and double labeling immunocytochemistry identified the constitutive expression of NgR in cultured human astrocytes. These results suggest that Nogo-A expressed on oligodendrocytes might interact with NgR presented by reactive astrocytes and microglia/macrophages in active demyelinating lesions of MS, although biologic effects caused by Nogo-A/NgR interaction among glial cells remain unknown.

Key Words: Axonal regeneration, Multiple sclerosis, Nogo-A, Nogo receptor, Oligodendrocytes, Reactive astrocytes

INTRODUCTION

The adult mammalian central nervous system (CNS) has an extremely limited capacity to regenerate axons following injury. The reduced regenerative ability is attributable to the progressive disappearance of growth-promoting factors or the increasing appearance of growth-inhibitory molecules during maturation of the CNS 1. Recently, Nogo is identified as a myelin-associated inhibitor for axonal regeneration (2, 3). The Nogo gene encodes three distinct isoforms, named Nogo-A, -B, and -C, derived by alternative splicing and promoter usage. All of these share a small segment composed of 66 amino acid residues located between the two putative transmembrane domains named Nogo-66, in the C-terminal region homologous to the members of reticulon protein family (2, 3). Nogo-A, the largest isoform, is predominantly expressed on oligodendrocytes and their processes with location in the innermost adaxonal and outermost myelin membranes (4, 5). Nogo-A is also identified in a subpopulation of neurons with the subcellular location chiefly in the endoplasmic reticulum (ER) and the Golgi complex, concentrated at the postsynaptic density (6–9). Nogo-B shows a ubiquitous distribution pattern, while Nogo-C, the shortest isoform, is enriched in skeletal muscle (4, 10). Nogo-A has at least two discrete regions with neuronal growth-inhibitory activities: one is located in the Nogo-A-specific region spanning amino acids 544–725 that restricts neurite outgrowth; the other, Nogo-66, has the capacity to induce growth cone collapse. Both regions assume different membrane topologies depending on cell types (11). Nogo-66 binds to a high affinity receptor NgR, a glycoprotein composed of a signal sequence, a leucine-rich repeat (LRR)-type N-terminal region (LRRNT), eight LRR domains, a cysteine-rich LRR-type C-terminal domain (LRRCT), a unique C-terminal domain, and a glycosylphosphatidylinositol (GPI) anchorage site responsible for accumulation in lipid rafts (12, 13). NgR expression is sufficient to confer sensitivity to Nogo-66 on otherwise insensitive cells (12). In contrast to Nogo-A, NgR is not identified on oligodendrocytes but is expressed constitutively in a subset of neurons and their axons, including cerebral cortical pyramidal neurons and cerebellar Purkinje cells (12, 14, 15). Signal transduction mediated by NgR depends on its association with the low-affinity nerve growth factor receptor $p75^{NTR}$, which also serves as a coreceptor for the Trk family of neurotrophin receptors. Recent studies showed that not only Nogo-66 but also myelin-associated glycoprotein (MAG) and oligodendrocyte-myelin glycoprotein (OMgp) bind to NgR and transduce neurite growth-inhibitory signals via $p75^{NTR}$ by activating RhoA and inhibiting Rac1 (16, 17). By neutralizing anti-Nogo-A antibodies, NgR competitive antagonistic peptides, or soluble truncated NgR, in vivo blockade of the interaction between NgR and its

From the Department of Immunology (JIS, HO, TY), National Institute of Neuroscience, NCNP, Tokyo, Japan; and the Department of Neuropathology (KA), National Center Hospital for Mental, Nervous, and Muscular Disorders, NCNP, Tokyo, Japan.

Correspondence and reprints to: Jun-Ichi Satoh, MD, PhD, Department of Immunology, National Institute of Neuroscience, NCNP, 4-1-1 Ogawahigashi, Kodaira, Tokyo 187-8502, Japan. E-mail: satoj@ncnp.go.jp

Supported by grants from the Grant-in-Aid for Scientific Research (B2-15390280 and PA007-16017320), the Ministry of Education, Science, Sports and Culture, and the Organization for Pharmaceutical Safety and Research (OPS), Kiko, Japan.

JOBNAME: jnen 64#2 2005 PAGE: 2 OUTPUT: Mon December 27 15:05:19 2004
lww/jnen/93252/NEN19047

ligands induced long-distance axonal regeneration, compensatory sprouting, and upregulation of growth-associated genes. This was accompanied by enhancement of functional recovery after injury in the CNS (18–20).

Multiple sclerosis (MS) is pathologically characterized by multifocal inflammatory demyelination and axonal injury in the CNS white matter; the latter has been proposed as a principal cause of permanent disability in MS (21, 22). A recent study identified anti-Nogo-A autoantibody in the serum and cerebrospinal fluid of relapsing-remitting MS patients, suggesting a protective response to persistent demyelination and axonal damage (23). However, it remains unknown whether Nogo-A, MAG, and OMgp play an active role in interfering with axonal regeneration at the site of demyelinating lesions of MS. Previous studies suggested that Nogo-A in the intact adult rodent CNS regulates axonal plasticity and stabilizes major myelinated tracts to prevent the formation of aberrant fiber connections (24, 25). To investigate a physiological function of Nogo-A in development and maturation of the CNS, three independent lines of Nogo-A knockout mice have been established recently (26–28). Unexpectedly, all of these mice showed neither obvious neuroanatomic defects nor neurologic symptoms, indicating that Nogo-A is not pivotal for development and maintenance of axonal pathways at least in the absence of injury. Following spinal cord injury, some lines of Nogo-A-deficient mice showed an enhanced axonal regeneration of corticospinal tract fibers (26, 27). Importantly, inflammatory demyelination and axonal damage were less severe in Nogo-A-deficient mice affected with experimental autoimmune encephalomyelitis, an animal model of MS (29). Furthermore, NgR-deficient mice exhibited an enhanced axonal plasticity after ischemic stroke in the brain, accompanied by improved functional recovery (30). These observations suggest that Nogo-A and NgR interaction plays a central role in inhibition of axonal regeneration under pathologic conditions in the CNS.

In the present study, we have investigated the expression of Nogo-A and NgR in MS brains by immunohistochemistry. We found that Nogo-A expression was markedly upregulated in surviving oligodendrocytes at the edge of chronic active demyelinating lesions of MS, while NgR expression was greatly enhanced in reactive astrocytes and microglia/macrophages in these lesions. Our observations suggest a novel type of interaction between Nogo-A on oligodendrocytes and NgR on activated astrocytes and microglia at the site of demyelinating lesions of MS.

MATERIALS AND METHODS

MS and Control Brain Tissues

Ten-micron-thick serial sections were prepared from autopsied brains of 4 MS cases, 6 non-MS neurologic and psychiatric disease (OND) cases, and 6 neurologically normal control subjects listed in Table 1. Detailed clinical and neuroradiologic profiles of MS patients were described previously (31). The tissues were fixed with 4% paraformaldehyde or 10% neutral formalin and embedded in paraffin. Autopsies on all subjects were performed at the National Center Hospital for Mental, Nervous and Muscular Disorders, National Center of Neurology and Psychiatry (NCNP), Tokyo, Japan. Written informed consent was obtained in all cases. The present study was approved by the Ethics Committee of NCNP.

Immunohistochemistry and Immunocytochemistry

After deparaffinization, tissue sections were heated by microwave at 95°C for 10 minutes in 10 mmol/L citrate sodium buffer, pH 6.0. They were then treated at room temperature (RT) for 15 minutes with 3% H_2O_2-containing methanol. For $p75^{NTR}$ immunolabeling, the tissue sections

TABLE 1. MS and Control Cases Examined in the Present Study.

Case No.	Age (year) and Sex (male/female)	Diagnosis	Cause of Death
791	29 F	Secondary progressive multiple sclerosis	Asphyxia
744	40 F	Secondary progressive multiple sclerosis	Respiratory failure
609	43 F	Primary progressive multiple sclerosis	Hyperglycemia
544	33 M	Secondary progressive multiple sclerosis	Sepsis and multiorgan failure
719	47 M	acute cerebral infarction	Sepsis
786	84 M	Acute cerebral infarction	Disseminated intravascular coagulation
789	62 M	Old cerebral infarction	Pancreatic cancer
807	56 M	Old cerebral infarction	Myocardial infarction
523	36 F	Schizophrenia	Lung tuberculosis
826	61 M	Schizophrenia	Asphyxia
G6	79 F	Neurologically normal subject	Hepatic cancer
G7	75 F	Neurologically normal subject	Breast cancer
G8	60 F	Neurologically normal subject	External auditory canal cancer
G9	74 F	Neurologically normal subject	Gastric and hepatic cancers
A2623	83 F	Neurologically normal subject	Gastric cancer and myocardial infarction
A2647	65 M	Neurologically normal subject	Liver cirrhosis and bronchopneumonia

The present study includes four MS cases numbered 791, 744, 609, and 544, 6 non-MS neurologic and psychiatric disease cases (OND) numbered 719, 786, 789, 807, 523, and 826, and 6 neurologically normal cases (NNC) numbered G6, G7, G8, G9, A2623, and A2647.

JOBNAME: jnen 64#2 2005 PAGE: 3 OUTPUT: Mon December 27 15:05:20 2004
lww/jnen/93252/NEN19047

were pretreated with 0.125% trypsin solution (Nichirei, Tokyo, Japan) at 37°C for 10 minutes. They were incubated with 10% normal goat serum-containing phosphate-buffered saline (PBS) at RT for 15 minutes to block nonspecific staining. The sections were incubated in a moist chamber at 4°C overnight with primary antibodies listed in Table 2. After washing with PBS, they were labeled at RT for 30 minutes with peroxidase-conjugated secondary antibodies (Nichirei) followed by incubation with a colorizing solution containing diaminobenzidine tetrahydrochloride and a counterstain with hematoxylin. For negative controls, tissue sections were incubated with a rabbit negative control reagent (DAKO, Carpinteria, CA) instead of primary antibodies.

For immunocytochemistry, human astrocytes in culture on cover glasses were fixed with 4% paraformaldehyde in 0.1 mol/L phosphate buffer, pH 7.4 at RT for 10 minutes, followed by incubation with PBS containing 0.5% Triton X-100 at RT for 20 minutes. For double immunolabeling, the cells and tissue sections were incubated at RT for 30 minutes with a mixture of rabbit anti-NgR antibody and mouse anti-GFAP antibody. Then, they were incubated at RT for 30 minutes with a mixture of rhodamine-conjugated anti-rabbit IgG and FITC-conjugated mouse IgG (ICN-Cappel, Aurora, OH). After several washes, they were mounted with glycerol-polyvinyl alcohol and examined under a Nikon ECLIPSE E800 universal microscope equipped with fluorescein and rhodamine optics. Negative controls were processed following all the steps except for exposure to primary antibody. In some experiments, tissue sections were initially stained with rabbit anti-Nogo-A antibody, then followed by incubation with alkaline phosphatase-conjugated secondary antibody (Nichirei) and colorized with New Fuchsin substrate. After inactivation of all the antibodies by heating the sections at 95°C for 10 minutes in 10 mmol/L citrate sodium buffer, pH 6.0, they were relabeled with rabbit anti-MBP antibody, followed by incubation with peroxidase-conjugated secondary antibody (Nichirei) and colorized with diaminobenzidine tetrahydrochloride substrate.

Cell Culture and Expression of Transgenes

Cultured human astrocytes derived from human neuronal progenitor cells were maintained in Dulbecco's Modified Eagle's medium (Invitrogen, Carlsbad, CA) supplemented with 10% fetal bovine serum (FBS), 100 U/mL penicillin, and 100 μg/mL streptomycin (feeding medium), as described previously (31). To enrich the GPI-anchored proteins, astrocytes were incubated at 37°C for 3 hours in the serum-free Dulbecco's Modified Eagle's medium /F-12 medium (Invitrogen) supplemented with 5 U/mL phosphatidylinositol-specific

TABLE 2. Primary Antibodies Used for Immunochemistry and Western Blot Analysis

Antibody (clone name)	Supplier	Code	Origin	Immunogens	Antigen Specificity	Concentration Used for Immunohistochemistry	Concentration Used for Western Blotting
Nogo-A	Santa Cruz Biotechnology	sc-25600	Rabbit	Peptide composed of amino acids 700–1,000 mapping at the internal region of human Nogo-A	Nogo-A, not reactive with Nogo-B or Nogo-C	1:2,000 (100 ng/mL)	1:12,000 (16.7 ng/mL)
NgR	Chemicon	AB5615	Rabbit	Recombinant mouse NgR	NgR	1:2,000	1:4,000
$p75^{NTR}$ (ME20.4)	Sigma	N5408	Mouse	Human melanoma cell line	Low affinity nerve growth factor receptor p75	1:500 (46 μg/mL)	NA
APP (22C11)	Chemicon	MAB348	Mouse	Recombinant human APP	APP	1:200 (5 μg/mL)	NA
GFAP	Dako	N1506	Rabbit	Purified bovine spinal cord GFAP	GFAP	Prediluted	NA
GFAP (GA5)	Nichirei	422261	Mouse	Purified swine spinal cord GFAP	GFAP	Prediluted	NA
MBP	Dako	N1564	Rabbit	Purified human brain MBP	MBP	Prediluted	NA
NF (2F11)	Nichirei	412551	Mouse	Purified human brain NF protein	Human 70-kDa and 200-KDa NF	Prediluted	NA
CD68 (KP1)	Dako	N1577	Mouse	Lysosomal granules of human lung macrophages	CD68	Prediluted	NA
CD3 (PS1)	Nichirei	413241	Mouse	Recombinant human CD3 epsilon chain	CD3	Prediluted	NA
HSP60	Santa Cruz Biotechnology	sc-1052	Goat	Peptide mapping at the amino terminus of human HSP60	HSP60	NA	1:2,000 (100 ng/mL)

NgR, Nogo receptor; NTR, neurotrophin receptor; APP, amyloid precursor protein; GFAP, glial fibrillary acidic protein; MBP, myelin basic protein; NF, neurofilament; HSP60, 60-kDa heat shock protein; NA, not applied.

JOBNAME: jnen 64#2 2005 PAGE: 4 OUTPUT: Mon December 27 15:05:21 2004
lww/jnen/93252/NEN19047

phospholipase C (PI-PLC; Sigma, St. Louis, MO). The culture supernatant was harvested and concentrated at a 1/30 volume by centrifugation on a Centricon-10 filter (Millipore, Bedford, MA). Human cell lines such as HEK293 embryonal kidney cells, U-373MG astrocytoma, and NTera2 teratocarcinoma were obtained from the RIKEN Cell Bank (Tsukuba, Japan) and the American Type Culture Collection (Rockville, MD). In limited experiments, human astrocytes and U-373MG cells were incubated for 4 to 8 days in the serum-free Dulbecco's Modified Eagle's medium /F-12 medium supplemented with an insulin-transferrin-selenium supplement (Invitrogen) with or without inclusion of recombinant human IL-1β or TNFα (PeproTech EC, London, UK).

For expression of transgenes, the human *Nogo-A* gene (GenBank accession no. NM_020532) encoding the Nogo-A-specific segment (NAS; amino acids 186–1004) and the human *NgR* gene (NM_023004) encoding the full-length NgR after a cleavage of the N-terminal signal peptide (amino acids 27–473) were amplified by PCR using PfuTurbo DNA polymerase (Stratagene, La Jolla, CA) from cDNA of NTera2-derived human neurons (32) using sense and antisense primer sets (5'gatgagaccctttttgctcttcct3' and 5'tcatgaagttttactcagctctgctga3' for Nogo-A and 5'acgatggagagggcgtccgctggag3' and 5'gcagggcccaagcactgtccacagcac3' for NgR). The *Nogo-A* or *NgR* gene was cloned in an expression vector pcDNA4/HisMax-TOPO containing a N-terminal Xpress tag for detection of the recombinant protein or in pEF6/V5-His-TOPO containing a C-terminal V5 tag (Invitrogen), respectively. The vectors were transfected into HEK293 cells by using Lipofectamine 2000 reagent (Invitrogen). At 48 hours after transfection, the cells were processed for Western blot analysis.

For RT-PCR analysis, cDNA was amplified for 30 cycles by PCR using sense and antisense primer sets specific for the human NgR gene (5'cagtacctgaggctcaacgacaac3' and 5'acctgagccttctgagtcaccagt3'; product size 588 bp) or the human glyceraldehyde-3-phosphate dehydrogenase (*G3PDH*) gene (NM_002046; 5'ccatgttcg-tcatgggtgtgaacca3' and 5'gccagtagaggcagggatgatgttc3'; the product size 251 bp) (32).

Western Blot Analysis

To prepare total protein extract, the cells and tissues were homogenized in RIPA lysis buffer composed of 50 mmol/L Tris-HCl, pH 7.5, 150 mmol/L NaCl, 1% Nonidet P40, 0.5% sodium deoxycholate, 0.1% SDS, and a cocktail of protease inhibitors (Roche Diagnostics, Mannheim, Germany), followed by centrifugation at 12,000 rpm for 20 minutes at RT. The supernatant was collected for separation on a 6%, 8%, or 12% SDS-PAGE gel. The protein concentration was determined by a Bradford assay kit (BioRad, Hercules, CA). After gel electrophoresis, the protein was transferred onto nitrocellulose membranes and immunolabeled at RT overnight with rabbit anti-Nogo-A or anti-NgR antibody. The membranes were incubated at RT for 30 minutes with horseradish peroxidase-conjugated anti-rabbit IgG (Santa Cruz Biotechnology, Santa Cruz, CA). The specific reaction was visualized with a Western blot detection system using a chemiluminescent substrate (Pierce, Rockford, IL). After the antibodies were stripped by incubating the membranes at 50°C for 30 minutes in stripping buffer composed of 62.5 mmol/L Tris-HCl, pH 6.7, 2% SDS, and 100 mmol/L 2-mercaptoethanol, the membranes were processed for relabeling with goat anti-HSP60 antibody followed by incubation with horseradish peroxidase-conjugated anti-goat IgG (Santa Cruz Biotechnology), or with mouse monoclonal anti-Xpress or anti-V5 antibody (Invitrogen) followed by incubation with horseradish peroxidase-conjugated anti-mouse IgG (Santa Cruz Biotechnology).

RESULTS

Characterization of Anti-Nogo-A and Anti-NgR Antibodies

To characterize the specificity of polyclonal anti-Nogo-A antibody (sc-25600) and anti-NgR antibody (AB5615) (Table 2), we investigated Nogo-A and NgR expression in brain homogenates by Western blot analysis. The antibody sc-25600 was raised against a peptide consisting of amino acids 700–1,000 of the human Nogo-A that represents a Nogo-A-specific internal segment not shared with Nogo-B or Nogo-C. This antibody reacted with a single band of 190-kDa protein in human and mouse brain and spinal cord homogenates (Fig. 1A). This size corresponds to that of the full-length Nogo-A of the rat oligodendrocyte lysate (11). The antibody sc-25600 recognized a 140-kDa recombinant NAS protein with an Xpress tag in the vector-transfected HEK293 cells but did not react with any proteins in nontransfected HEK293 cells (Fig. 1C). The antibody AB5615 was raised against a recombinant mouse NgR. This antibody reacted with a 64-kDa protein in human and mouse brain and spinal cord homogenates (Fig. 1B). This size corresponds to that of the full-length NgR identified in the NgR gene-transfected CHO-K1 cells and SH-SY5Y cells (33, 34). The antibody AB5615 recognized not only a 64-kDa endogenous NgR protein constitutively expressed in nontransfected HEK293 cells but also reacted with several bands immunoreactive for a V5 tag in the vector-transfected HEK293 cells (Fig. 1D). The latter might represent posttranscriptionally modified NgR isoforms. In agreement with detection of NgR in HEK293 cells on immunoblot, RT-PCR analysis using NgR-specific primer sets, which do not amplify NgR homologues NgR111 and NgR112 (33), identified the constitutive expression of NgR mRNA in HEK293 cells (data not shown). [F1]

Nogo-A Expression on Oligodendrocytes in Demyelinating Lesions of MS

To investigate Nogo-A expression in MS lesions, the brain, spinal cord, and optic nerve sections of 4 progressive MS patients and 12 non-MS control cases (Table 1) were processed for immunohistochemistry using the antibody sc-25600. Adjacent sections were stained with the antibodies against cell type-specific markers. In all MS cases, a substantial population (20%–60%) of surviving oligodendrocytes and remaining myelin sheath at the edge of chronic active demyelinating lesions, where numerous CD68+ macrophages/microglia accumulated (Fig. 2a inset), expressed an intense immunoreactivity for Nogo-A (Table 3; Figure 2a and 2b inset). In contrast, a smaller population (<20%) of oligodendrocytes [F2] [T3]

JOBNAME: jnen 64#2 2005 PAGE: 5 OUTPUT: Mon December 27 15:05:21 2004
lww/jnen/93252/NEN19047

distributed in the white matter of the brains of neurologically normal subjects displayed a fairly weak immunoreactivity for Nogo-A (Fig. 2e). An intense Nogo-A immunoreactivity was also found in surviving oligodendrocytes at the lesion border of acute and old cerebral infarction (Fig. 2d inset). The number of Nogo-A-expressing oligodendrocytes was much smaller in the center of demyelinating lesions and in the normal-appearing white matter of MS brains (Fig. 2d) and in the necrotic lesions of cerebral infarction. Double labeling immunohistochemistry verified a close association between Nogo-A-expressing oligodendrocytes and MBP, an interacting partner of Nogo-A (35) in MS lesions (Fig. 2b inset). In all MS and non-MS cases, variable Nogo-A immunoreactivity was identified in a small population (<20%) of neurons widely distributed in the whole CNS, including motor neurons in the spinal cord with its location in the perikarya and neurites (Table 3; Fig. 2f), suggesting that not all but a substantial population of neurons in the adult human CNS express Nogo-A constitutively. In contrast, Nogo-A expression was undetectable in GFAP$^+$ reactive astrocytes (Fig. 2a, c), CD68$^+$ microglia/macrophages, ependymal cells, or CD3$^+$ T lymphocytes in chronic active demyelinating lesions of MS, ischemic lesions of cerebral infarction, and other cases (Table 3).

To investigate a possible association of Nogo-A-expressing oligodendrocytes with damaged axons in active MS lesions, adjacent sections were stained with the antibody against amyloid precursor protein (APP), a sensitive marker for acute axonal injury (21). However, APP-immunoreactive [F3] axons were hardly detectable in any cases examined (Fig. 3b), and these axons did not colocalize with Nogo-A-expressing [AU1] oligodendrocytes (not shown).

NgR Expression on Reactive Astrocytes and Microglia in Demyelinating Lesions of MS

To investigate NgR expression in MS lesions, the brain, spinal cord, and optic nerve sections of 4 MS patients and 12 non-MS control cases (Table 1) were processed for immunohistochemistry using the antibody AB5615. In all MS and cerebral infarction cases, a large population (>60%) of GFAP$^+$ reactive astrocytes and CD68$^+$ microglia/macrophages that accumulated in chronic active and inactive demyelinating lesions or in ischemic lesions expressed an intense immunoreactivity for NgR (Table 3; Fig. 4a, d, e). Furthermore, a fairly [F4] small number of GFAP$^+$ astrocytes and CD68$^+$ microglia, occasionally found in the brains of neurologically normal subjects, were also stained intensely with anti-NgR antibody (Fig. 4d inset). These observations suggest that both astrocytes and microglia express high levels of NgR, particularly when they become activated. Double-labeling immunohistochemistry verified coexpression of NgR and GFAP on reactive astrocytes in demyelinating lesions of MS (Fig. 3c, d). In all MS and non-MS cases, variable NgR immunoreactivity was identified in a large population (>60%) of neurons and their neurites widely distributed in the whole CNS (Table 3; Fig. 4f), suggesting that not all but a wide variety of neurons in the adult human CNS constitutively express high levels of NgR. Among them, cerebral cortical neurons and spinal cord motor neurons coexpressed Nogo-A and NgR (Figs. 2f, 4f). In addition,

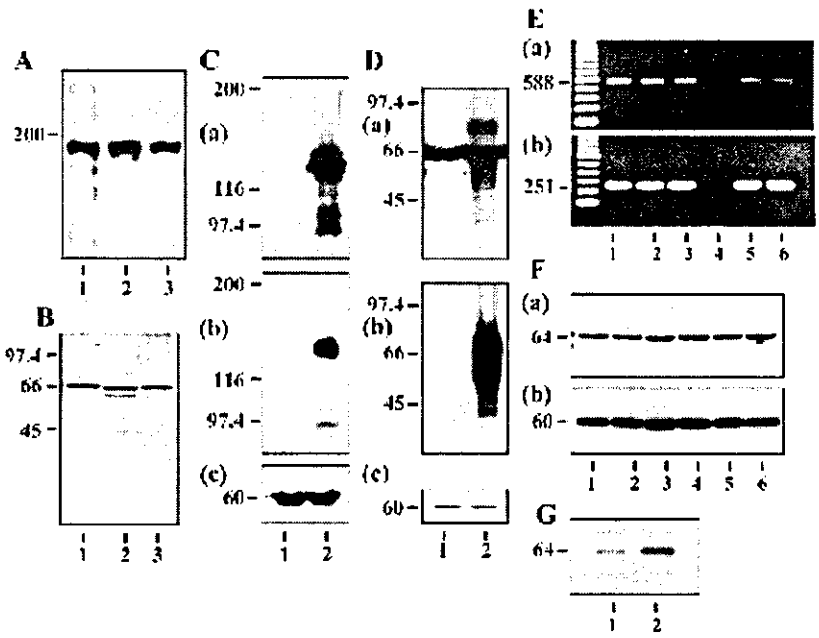

FIG. 1. Nogo-A and NgR expression in human brain, cultured astrocytes, transfected HEK293 cells. (**A, B**) Immunoblot of brain homogenates with anti-Nogo-A (**A**) or anti-NgR (**B**) antibody. Human (lane 1) or mouse brain (lane 2), and mouse spinal cord (lane 3), 20 μg of protein each. (**C, D**) Immunoblot of HEK293 cells expressing Nogo-A-specific segment (NAS) (**C**) or NgR (**D**) with (**Ca**) anti-Nogo-A, (**Cb**) anti-Xpress, (**Da**) anti-NgR, (**Db**) anti-VS, or (**Cc** and **Dc**) anti-HSP60 antibody. Nontransfected (lane 1) and transfected (lane 2) HEK293 cells, 120 μg (**C**) or 4 μg (**D**) of protein each. E: RT-PCR analysis of (**Ea**) NgR and (**Eb**) G3PDH mRNA in human astrocytes, astrocytoma, and teratocarcinoma cell lines. The cells were incubated for 8 days in serum-free (lanes 2, 5) or 10% FBS-containing (lanes 1, 3, 4, 6) medium, with (lanes 1–3, 5, 6) or without (lane 4) inclusion of RT step. NTera2 (lane 1), cultured human astrocytes (lanes 2–4), and U-373MG (lanes 5, 6). (**F**) Immunoblot of cultured human astrocytes with (**Fa**) anti-NgR or (**Fb**) anti-HSP60 antibody. The cells were incubated for 4 days in serum-free (lanes 1–3) or 10% FBS-containing (lanes 4–6) medium with inclusion of 100 ng/mL IL-1β (lanes 2, 5) 100 ng/mL TNF-α (lanes 3, 6) or without cytokines (lanes 1, 4), 30 μg of protein each. (**G**) Immunoblot of supernatant of cultured human astrocytes with anti-NgR antibody. The supernatant of (lane 1) untreated and (lane 2) PI-PLC-treated astrocytes.

JOBNAME: jnen 64#2 2005 PAGE: 6 OUTPUT: Mon December 27 15:05:27 2004
lww/jnen/93252/NEN19047

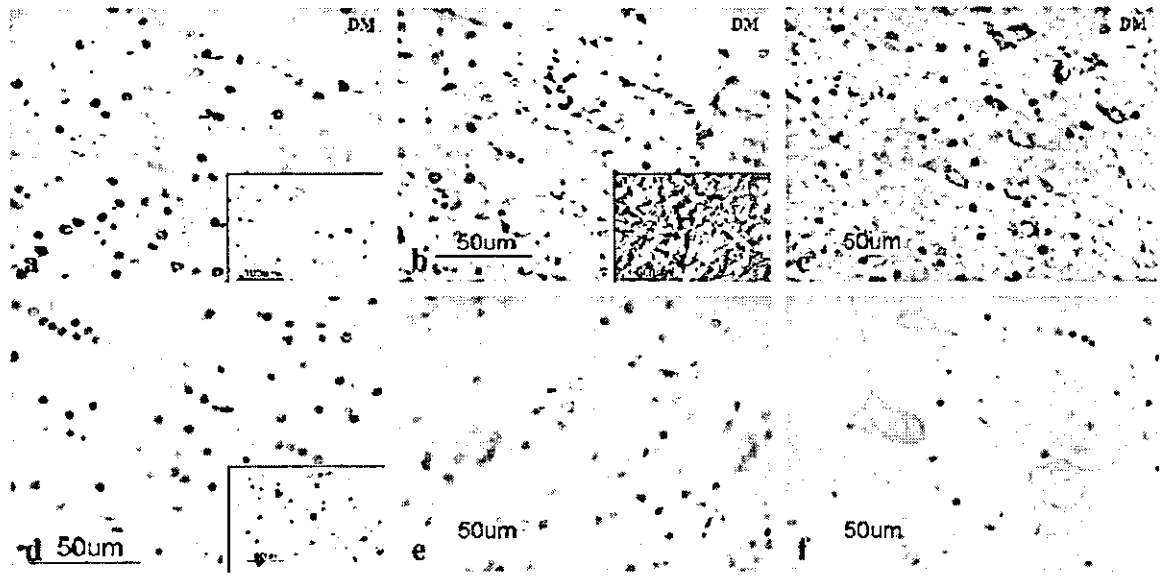

FIG. 2. Nogo-A expression on oligodendrocytes in demyelinating lesions of MS. Immunohistochemistry. (**a**) No. 744 MS, Nogo-A, the edge of chronic active demyelinating lesions (DM) in the subcortical white matter of the frontal lobe (inset, CD68). (**b**) No. 744 MS, MBP, the adjacent section of panel a (inset, no. 791 MS, double immunolabeling for Nogo-A as red and MBP as brown). (**c**) No. 744 MS, GFAP, the adjacent section of panel a. (**d**) No. 744 MS, Nogo-A, the normal-appearing white matter of the frontal lobe (inset, no. 786 acute cerebral infarction, Nogo-A, the lesion border in the subcortical white matter of the parietal lobe). (**e**) No. A2647 neurologically normal subject, Nogo-A, the subcortical white matter of the frontal lobe. (**f**) No. 791 MS, Nogo-A, motor neurons in the spinal cord.

ependymal cells constitutively expressed intense NgR immunoreactivity, while NgR expression was not found in oligodendrocytes (Table 3; Fig. 4a, c) or CD3$^+$ T lymphocytes.

In contrast to widespread distribution of NgR in the human CNS, the NgR coreceptor $p75^{NTR}$ immunoreactivity was identified in fairly restricted regions: most prominently expressed in nerve fibers of substantia gelatinosa in the spinal cord (Fig. 3a), tractus solitarius in the brainstem, and found in the vascular wall in the cerebrum. $p75^{NTR}$ was not expressed on oligodendrocytes, astrocytes, or microglia/macrophages in any cases examined (not shown).

Constitutive Expression of NgR in Cultured Human Astrocytes

Because a previous study did not identify NgR on astrocytes in the human CNS (15), NgR expression was studied in cultured human astrocytes to verify the present observations. RT-PCR analysis using NgR-specific primer sets identified a substantial level of NgR mRNA in human astrocytes in culture, along with U-373MG and NTera2 cells (Fig. 1E). No products were amplified when total RNA was processed for PCR omitting RT step, confirming that a contamination of genomic DNA was excluded (Fig. 1E). By Western blot analysis, NgR protein levels were unaltered in cultured human astrocytes by exposure to IL-1β or TNFα under the serum-free or serum-containing culture condition, when standardized against the levels of HSP60, a housekeeping gene product, detected on the identical blots (Fig. 1F). Double labeling immunocytochemistry verified coexpression of NgR and GFAP in cultured human astrocytes, where a substantial NgR immunoreactivity was identified in the cytoplasm (Fig. 3d–f). Furthermore, a large amount of NgR protein was detected in the supernatant of PI-PLC-treated

TABLE 3. Differential Expression of Nogo-A and Nogo Receptor in Glial Cells and Neurons in MS and Control Brains

Brain	Astrocytes			Microglia/Macrophages			Oligodendrocytes			Neurons		
	MS	OND	NNC	MS	OND	NNC	MS	OND	NNC	MS	OND	NNC
Nogo-A	n(−)	n(−)	n(−)	n(−)	n(−)	n(−)	m(++)	m(++)	s(+)	s(+/++)	s(+)	s(+)
NgR	l(++)	l(++)	l*(++)	l(++)	l(++)	l*(++)	n(−)	n(−)	n(−)	l(+/++)	l(+/++)	l(+/++)

The present study includes 4 MS cases, 6 non-MS neurologic and psychiatric disease cases (OND), and 6 neurologically normal cases (NNC), as shown in Table 1. The population size of immunoreactive cells per total is expressed as [l] large (>60%); [m] moderate (60–20%); [s] small (<20%); [n] almost none; and [l*] large population but small number. The intensity of immunoreactivity is graded as (−) negative, (+) weak, (++) intense, and (+/++) variable

Fig. 2 live 4/C

JOBNAME: jnen 64#2 2005 PAGE: 7 OUTPUT: Mon December 27 15:05:37 2004
lww/jnen/93252/NEN19047

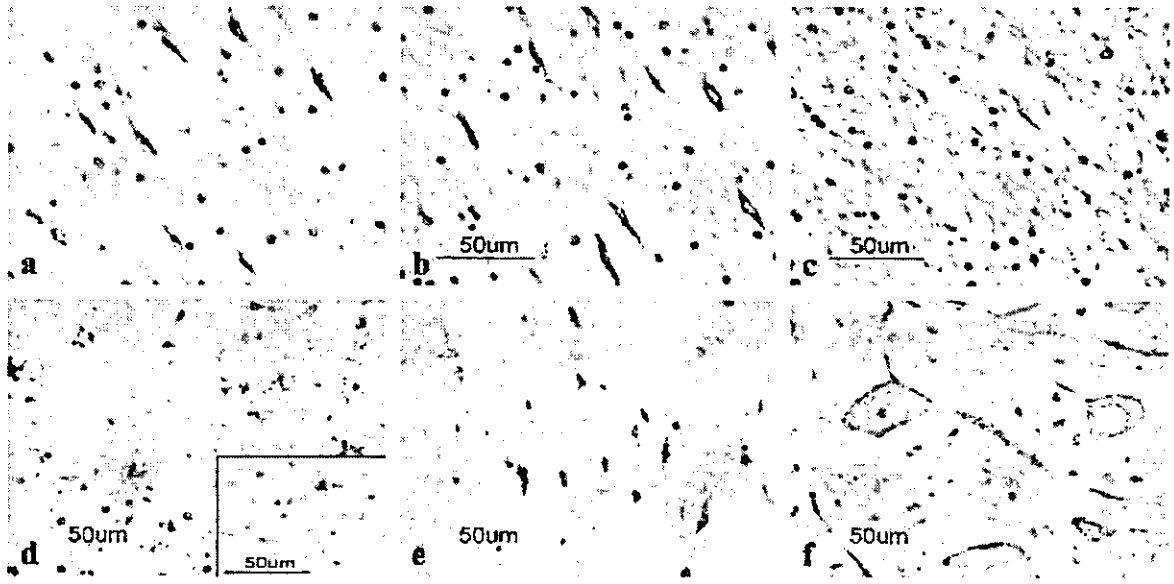

FIG. 3. Coexpression of NgR and GFAP on reactive astrocytes in MS lesions and cultured human astrocytes. Immunohistochemistry and immunocytochemistry. (a) No. 791 MS, $p75^{NTR}$, the substantia gelatinosa in the spinal cord. (b) No. 609 MS, APP, chronic active demyelinating lesions in the medulla oblongata. (c, d) No. 744 MS, double immunolabeling for NgR (red) and GFAP (green), chronic active demyelinating lesions in the subcortical white matter of the frontal lobe. (e, f) Cultured human astrocytes, double immunolabeling for NgR (red) and GFAP (green).

human astrocyte cultures (Fig. 1G), although a small amount of NgR was found in that of untreated cultures (Fig. 1G).

DISCUSSION

The present study showed that Nogo-A expression was markedly upregulated in surviving oligodendrocytes, while NgR expression was greatly enhanced in reactive astrocytes and microglia/macrophages in chronic active demyelinating lesions of MS and ischemic lesions of acute and old cerebral infarction, when compared with their expression in the brains of neurologically normal controls. Both Nogo-A and NgR were also identified in a subpopulation of neurons in the brain and spinal cord, consistent with previous observations (4–9, 14, 15). In contrast, Nogo-A was undetectable in reactive astrocytes and microglia/macrophages, and NgR was not virtually expressed on oligodendrocytes. Previous studies suggested that Nogo-A released from injured oligodendrocytes and damaged myelin sheath in the CNS lesions acts on neighboring NgR-expressing neurons and their axons (36). Our observations raise an alternative possibility that Nogo-A expressed on surviving oligodendrocytes interacts directly with NgR presented by reactive astrocytes and microglia/macrophages at the site of active demyelinating lesions of MS. A possible role of NgR on reactive astrocytes and microglia includes an inhibition of their proliferation, down-regulation of cytokine production, and sequestration of Nogo-A released from damaged oligodendrocytes by acting as a non-functioning decoy receptor.

The regulatory mechanism for Nogo-A and NgR expression remains largely unknown. Several studies suggested that Nogo-A and NgR levels are not substantially altered in the adult rodent CNS following injury (4, 6, 14). The CNS injury is often accompanied by a local infiltration of lymphocytes and macrophages and an activation of microglia and astrocytes, all of which provide a source of reactive oxygen species, pro-inflammatory cytokines, and neurotrophic factors. Previously, we found that Nogo-A and NgR mRNA levels are unaffected in human neurons in culture by exposure to basic FGF, BDNF, GDNF, IL-1β, or TNF-α, despite their expression of specific receptors (32). The present study revealed that human astrocytes in culture constitutively express NgR, whose levels remain unchanged by treatment with IL-1β or TNFα. Recent studies showed that the expression of Nogo-A but not of NgR is regulated by stress-inducing stimuli. Global ischemia enhances Nogo-A expression on the myelin sheath in the adult rat brain (37), supporting the present observations. In contrast, neonatal hypoxia reduces Nogo-A protein levels on oligodendrocytes in a mouse model (38). Nogo-A expression is markedly reduced at CNS paranodes in the rats affected with experimental autoimmune encephalomyelitis (39). Nogo-A expression is upregulated around the lesion site, whereas NgR is maintained at constant levels in the adult mouse and rat spinal cord following injury (5, 8). Nogo-A mRNA levels are elevated in the adult rat hippocampal neurons after kainate-induced seizure (40). Furthermore, Nogo-A is induced in hippocampal neurons of the patients with temporal lobe epilepsy (41). Nogo-A is upregulated in denervated and innervated mouse skeletal muscle and in postmortem and biopsied muscles of amyotrophic lateral sclerosis patients (42, 43).

The human Nogo-A/B promoter lacks a typical TATA-box and consensus sequences for known oligodendrocyte-specific

Fig. 3 live 4/C

JOBNAME: jnen 64#2 2005 PAGE: 8 OUTPUT: Mon December 27 15:05:46 2004
lww/jnen/93252/NEN19047

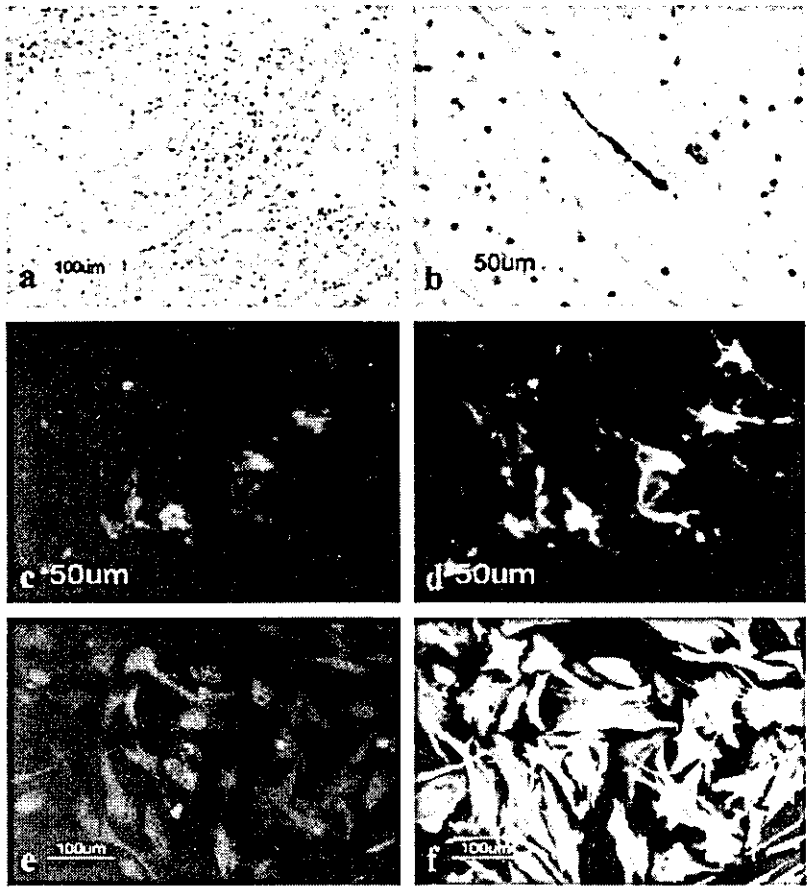

FIG. 4. NgR expression on reactive astrocytes and microglia in demyelinating lesions of MS. Immunohistochemistry. **(a)** No. 744 MS, NgR, the edge of chronic active demyelinating lesions in the subcortical white matter of the frontal lobe. **(b)** No. 744 MS, GFAP, the adjacent section of panel a. **(c)** No. 744 MS, MBP, the adjacent section of panel a. **(d)** No. 791 MS, NgR, chronic active demyelinating lesions in the pons (inset, no. A2647 neurologically normal subject, NgR, the subcortical white matter of the frontal lobe). **(e)** No. 744 MS, NgR, chronic active demyelinating lesions in the pons. **(f)** No. 744 MS, NgR, motor neurons in the spinal cord.

transcription factors, but it has a CpG island where a number of CpG sequences are frequently methylated (10). Such GC-rich promoters are typically identified in housekeeping genes whose expression is ubiquitous. However, multiple GC-boxes within the promoter region might lead to a synergistic activation by the Sp1 family of oligodendrocyte-specific or neuron-specific transcription factors (10). Interestingly, several nonneural cell lines such as 3T3 fibroblasts and C2 myoblasts express Nogo-A, where no direct correlation is observed between Nogo-A mRNA and protein levels (10). On the other hand, the human NgR promoter has not at present been characterized. An in situ hybridization study showed that NgR is undetectable in the spinal cord, and not expressed in ependymal cells, but identified in a subpopulation of neurons in the neocortex, hippocampus, amygdala, and the dorsal root ganglia in the adult human CNS (15). The discrepancy between this study and our own is attributable to the differences in brain tissues examined and the methods applied for identification of NgR. Recent studies showed that a subset of CNS neurons, including motor neurons in the adult rat and mouse spinal cord, coexpress NgR and Nogo-A (4, 8, 14), supporting the present observations. In addition, both Nogo-A and NgR are identified in the human spinal cord during development when Nogo-A does not play a negative role in regeneration (44). Most importantly, NgR expression is not confined to neurons. U87MG human glioblastoma cells express a great amount of endogenous NgR, through which Nogo-66 modulates their growth and migration (45). Although the LRR, LRRCT, and LRRNT subdomains of NgR are all involved in ligand binding (46), the DNAQLR motif located in the third LRR domain is identified as the principal epitope recognized by a monoclonal anti-NgR antibody capable of blocking binding of all NgR ligands (47). We found that a substantial NgR immunoreactivity was located in the cytoplasm of cultured human astrocytes, in addition to the detection of NgR protein in the supernatant of PI-PLC-treated and untreated cultures. The intracellular localization of NgR appears unusual, but it might reflect the changes in cell–cell interactions under culture conditions (44). Supporting our observations, an immunoelectron microscopic analysis showed that NgR is located at both presynaptic and postsynaptic regions where NgR-immunoreactive products distribute diffusely among cytoplasmic elements including synaptic vesicles, mitochondria, and microtubules (5). Furthermore, in human neuroblastoma cells, NgR is constitutively cleaved in a post-ER compartment by zinc metalloproteinases, and a

Fig. 4 live 4/C